INSTITUTE OF PHYSICS PUBLISHING METROLOGIA

Metrologia **43** (2006) S31–S35 doi:10.1088/0026-1394/43/2/S07

NIST reference cryogenic radiometer designed for versatile performance

J M Houston and J P Rice

National Institute of Standards and Technology, Gaithersburg, MD, USA

Received 20 October 2005
Published 23 March 2006
Online at stacks.iop.org/Met/43/S31

Abstract
We describe the concept of modularity and versatility in the construction of a new cryogenic radiometer developed at the National Institute of Standards and Technology. We address the benefits of the modular design in the construction and development and discuss some of the device characterizations and results of a cryogenic radiometer intercomparison.

1. Introduction

Cryogenic electrical substitution radiometers presently provide the basis for optical measurements in most national measurement institutes. The National Institute of Standards and Technology (NIST) required a new cryogenic radiometer that would provide the lowest possible uncertainty and yet would not become quickly obsolete. The new radiometer needed to have the versatility to grow with NIST's needs, to embrace new technologies and be able to provide laser power measurements with uncertainties of 0.01% or better over a range of power levels from microwatts to milliwatts. Additionally, the radiometer needed to have an improved thermal performance and the ability to calibrate a variety of optical detectors.

2. Design

The cryogenic radiometer that was designed and built at NIST is called the primary optical watt radiometer (POWR), previously known as HACR 2. POWR has replaced the high accuracy cryogenic radiometer (HACR) [1, 2]. While POWR measures optical power responsivity of detectors using lasers, the unique element of the NIST design is the concept of modularity. The radiometer can be divided into three main sections, each of which has design elements that contribute to the versatility of POWR.

The cryostat has been designed as a platform for the cryogenic radiometric measurements. It is optimized for thermal performance yet able to support various optical detector and thermometry configurations. The measurement versatility comes from the series of threaded holes in the base of the helium reservoir, which is a 381 mm diameter plate called the cold plate. The critical experimental elements are thermally anchored to the cold plate and are easily removed or replaced. A series of wiring paths that support the different types of four-wire heaters and thermometry and two-wire thermometry are connectorized inside the radiometer for ease of removal. One final element in the actual cryostat design is that it can be operated at two different temperatures, at 4.2 K for most measurements and at 2 K to reduce the thermal noise in the measurement of significantly lower optical powers.

The detector module design is critical in that the goal was to achieve laser power measurements with 0.01% uncertainty at the microwatt and milliwatt power levels and yet be able to change receiver cavities. The detector module design comprises four main elements: the cold block, the thermal anchor, the heat sink and the receiver cavity. The receiver cavity and the thermal anchor were specifically designed with the ability to measure microwatt to milliwatt optical power with 0.01% uncertainties or better. The heat sink design includes a place to mount the thermal anchor and a 20 mm diameter receiver cavity combination, and a limiting entrance aperture. Heaters and thermometers on the heat sink regulate its temperature to reduce the noise and uncertainty in the receiver cavity's measurements. The receiver cavity/heat sink module is then mounted onto the cold block. The main purpose of the cold block is to provide a liquid-helium-temperature background that surrounds the receiver cavity. The cold block is the part of the detector module that attaches to the cold plate and is thermally anchored to the liquid helium reservoir.

A baffle section which is attached to the cold plate and in front of the detector module is designed to limit the receiver cavity's field of view and to measure the scatter in the laser beam. There are locations in the front optics sections to add extra apertures to additionally limit the receiver cavity's field of view.

The front optics section includes the window section. Besides the Brewster angle window, this front optics section design provides the opportunity to measure the window

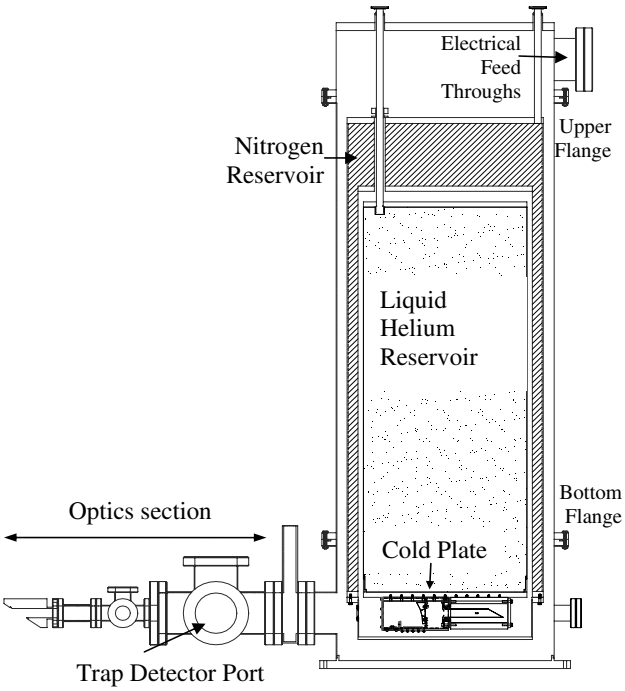

Figure 1. Side view of POWR. Starting from left to right is the front optics section that attaches to the conflat flange of the cryostat. In the cryostat a liquid nitrogen reservoir surrounds the liquid helium reservoir. The detector module and baffle section are attached to the bottom of the helium reservoir called the cold plate.

transmittance *in situ*. Attached between the window and the cryostat is a large, five-way cross. This cross is the location for a trap detector to be inserted to measure the transmittance of an installed window.

3. Construction

POWR can be disassembled easily into different sections. Each section is a single entity that can be modified or possibly replaced and then reassembled. In POWR this ability was designed and built into each of the main sections: the detector module, the baffle section and the front optics section.

3.1. The cryostat

The cryostat is designed and tested for improved mechanical and thermal performance. As shown in figure 1 the outer cryostat shell separates in two places, first at the top flange by the electrical to vacuum feedthroughs and second at the bottom flange by the cold plate. The upper flange allows access to the feedthroughs for wiring purposes and the lower flange allows access to the cold plate to exchange detector modules or for modifications.

The cryostat has a helium reservoir that holds nearly 100 L of liquid helium to provide a measured hold time of 14 days for normal operation. An annular reservoir of liquid nitrogen surrounds the helium reservoir for thermal insulation. The base of the helium reservoir, called the cold plate, is made of 304 stainless steel with helicoils for long-term mechanical performance (figure 2). On the cold plate there is an array of threaded holes to mount the detector

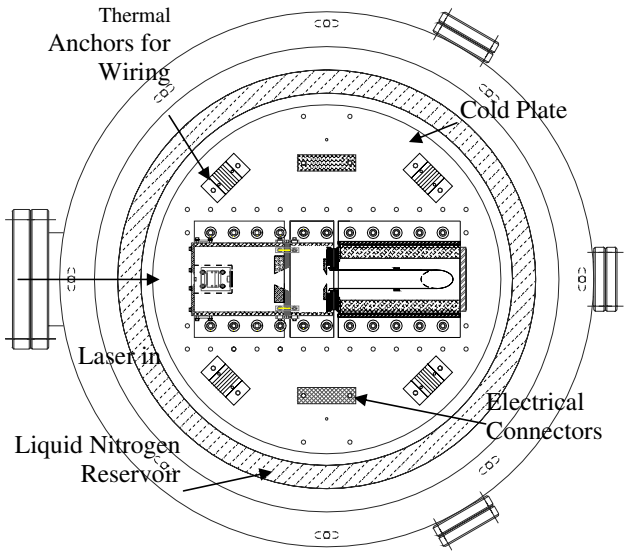

Figure 2. The cold plate provides a grid of threaded holes to mount all critical experimental components. The detector module and baffle section are mounted from right to left onto the cold plate. The laser beam enters from the left through the baffle section into the receiver cavity. Four thermal anchors for the wiring and two thermal anchors for the wire connectors are on the perimeter of the cold plate.

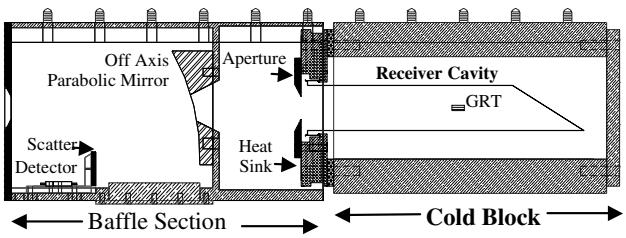

Figure 3. The detector module is on the right half with the receiving cavity mounted onto the thermal anchor and heat sink and surrounded by the cold block. On the left side is the baffle section with the off-axis parabolic mirror and silicon photodiode combination.

module and baffle section, with hole patterns set around the outer diameters for the thermometry, electrical connectors and thermal anchoring of wires. The detector module, baffle section and a surrounding 4.2 K shield are mounted onto the central portion of the cold plate. A 77 K shield attached to the bottom of the annular nitrogen reservoir further insulates the core elements. The detector module wiring that starts from the cold plate, travels through the shielding, up to the vacuum feedthroughs, is phosphor bronze. This cryostat feedthrough wiring configuration is kept the same for different detector modules.

3.2. The detector module

The detector module itself is shown in figure 3. The receiver cavity is an electroformed copper cylinder, 20 mm in diameter and 150 mm long. A 30° slant closes off the back end of the cavity. The inside of the cavity is coated with a specular black paint. One heater is non-inductively wrapped on the closed end of the cavity, with another two chip heaters attached to the back slant. Two germanium resistance thermometers (GRTs)

are located on the cylinder barrel. All wiring from the detector module ends in connectors to provide easy detachment. A Kapton[1] thermal anchor attaches the receiver cavity to the heat sink. Both the heat sink and the cold block are made of OFHC copper that is plated first with nickel and then gold. All surfaces are highly polished and reflective to reduce any radiative effects.

The detector module is constructed in two sections. The first section consists of a receiver cavity, a thermal link and a heat sink flange with its requisite wiring as the core of a distinct detector module. The second section consists of the cold block pieces that are used for each different detector module. In order to change a detector module, the receiver and heat sink combination is detached where the heat sink flange meets the cold block and then is replaced with another. The module integrity is maintained as long as the receiver cavity to heat sink combination is not altered.

While the main part of the detector module itself remained unchanged, the receiver cavity and some thermometry evolved until POWR achieved the desired performance. New receiver cavities were developed until there was one with the desired time constant and absorptance. The final receiver cavity that is used in the characterizations and calibrations described is termed Detector Module 3. An improvement in Detector Module 3 is that the wiring was changed to provide the capability for a feed-forward temperature control loop algorithm [3, 4].

3.3. The baffle section

One element designed into the measurement is the determination of the light scatter magnitude. This was achieved by placing a baffle section, located directly in front of the detector module, attached to the cold block (figure 3) and additional baffles along the interior optical path. The baffle section collects the scattered radiation with an off-axis parabolic mirror that surrounds the laser beam and reflects the scattered radiation into a silicon photodiode for measurement. The mirror has a hole in its centre to allow the laser beam to pass through.

The baffle section also has a modular design. Presently the collecting mirror and silicon detector are optimized for the visible wavelength range. Both can be replaced with an appropriately coated, higher reflectivity mirror and spectrally responsive detector for the UV or infrared regions of the spectrum. The mirror and the silicon photodiode, which is epoxied to a mount, are attached to the baffle section by screws. The Si detector can be optimally aligned to the plane of the mirror's focus by viewing the beam through an opening in the baffle section. This adjustment is done outside the cryostat by optically filling the mirror and adjusting the detector mount to the point of the focus. Once adjusted, the baffle section can be installed onto the cold plate.

[1] Certain commercial equipment, instruments or materials are identified in this paper to foster understanding. Such identification does not imply recommendation or endorsement by the NIST nor does it imply that the materials or equipment identified are necessarily the best available for the purpose.

4. Measurements

POWR, using Detector Module 3, was tested using two types of measurements. The first set was a series of characterizations to determine the uncertainty of this radiometer. Another series of measurements was the calibration of trap detectors for an intercomparison with other cryogenic radiometers.

4.1. The characterization of POWR

The receiver cavities for the detector modules, after being painted and built, were measured outside the cryostat for reflectance at three different wavelengths. The absorptance A was calculated using $A = 1 - \rho_c$, where ρ_c is the determined cavity reflectance. The receiver cavity reflectance was measured using an integrating sphere that was configured with three ports: two that were 180° apart for the passage of the laser beam and a third port perpendicular to that beam for a photodiode to measure the reflected signals. In order to eliminate the fluctuations of the source, all the reflectance measurements from the integrating sphere were ratioed to the simultaneous signals from a monitor detector of the laser beam. The cavity reflectance was determined using the following ratios in equation (1) where ρ_r is the ratio of the measured signal with the receiver cavity placed at the sphere's exit port to the monitor, ρ_s is the ratio with a NIST PTFE standard [5] at the sphere's exit port to the monitor and ρ_b is the ratio of the background in the integrating sphere with no blocking at the exit port to the monitor. The black receiver cavity absorbed most of the input laser beam and the room background was small, so the resulting ratios for ρ_r and ρ_b range from 1 ppm to 6 ppm. As a result $\rho_s \gg \rho_r$ or ρ_b, ρ_c is extremely small, and $A \approx 1$. The final cavity had absorptances of 0.999 995 at 633 nm, with the resulting uncertainties in the ρ_c a small contribution to POWR's uncertainty budget. Because the radiometer is versatile, the detector module can easily be removed and tested over time to see if the paint and absorptance are stable.

$$\rho_c = (\rho_r - \rho_b)/\rho_s. \tag{1}$$

Additional characterization measurements on the non-equivalence between the electrical and optical heating, the window transmittance and the electrical power scale are almost complete. A full discussion of POWR and its characterization is to be presented in a future paper.

4.2. Trap calibrations

The second type of measurements performed on POWR was the calibration of silicon trap detectors. The calibration of the trap detectors was performed in two different configurations, one with the traps on a separate translation stage in front of the window and a second with the trap detectors in the optical plane of the receiver cavity on the translation stage that moves the radiometer itself (figure 4). In the end, the second configuration was used for the trap calibration and the radiometer intercomparison.

For the trap calibration uncertainties the transmittance of the Brewster-angle cryostat window was measured *in situ* but not in vacuum. The Brewster-angle window was optimized for 633 nm and maintained in that alignment for the calibrations.

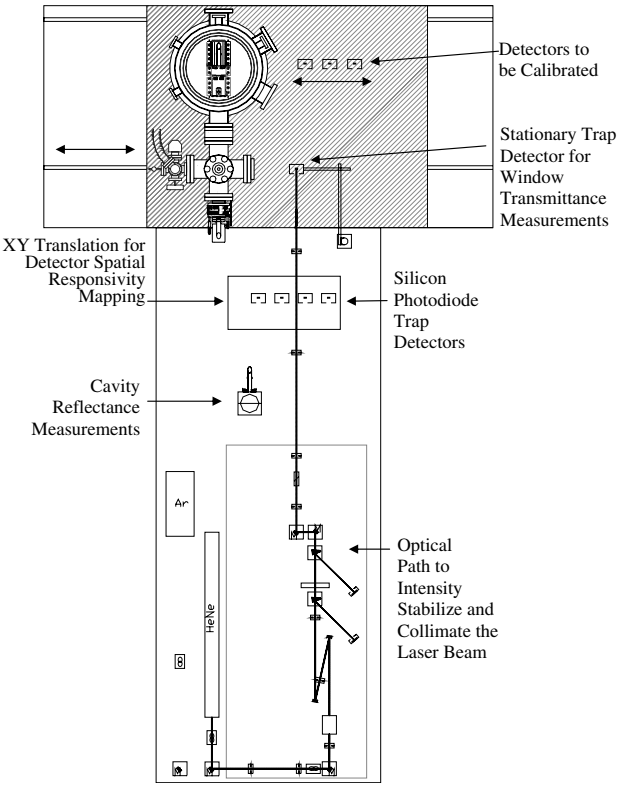

Figure 4. POWR facility layout shows the laser and optics area, the receiver cavity/trap characterization area and POWR on its translation stage. The bottom of the 'T' provides a location to set up lasers, to import fibre optics from SIRCUS and to clean and intensity-stabilize the beam. Characterization measurements of the detectors and receiver cavities using the lasers occur in the top of the 'T' stem. The optical path shown in the bottom stem portion of the table uses mainly mirror optics to collimate and intensity-stabilize the laser beams. The horizontal section supports a translation stage for the POWR cryostat and the detectors to move into the stabilized laser beam.

The transmittance measurements required the modularity of the POWR design and the usage of the translation stages in the facility to measure the window *in situ* and aligned. After an aligned POWR was translated out of the optical axis, a trap detector, located in a stationary portion of the optics table, was aligned to the laser beam. The trap detector was not only aligned to the beam but situated in a location where it slid into the opened trap detector port of POWR's optics section that is shown in figure 1. First POWR was moved out of the beam for the trap detector to measure the laser power. After the 'no window' measurement was complete, POWR was translated into its aligned position with the front optics section sliding over the trap detector (figure 4). The trap detector was translated vertically to correct for the beam displacement due to the window, and the transmittance measurements were made. All measurements were ratioed to the monitor detector on the laser beam to account for any beam fluctuations. The window transmittance is the ratio of the 'window in' ratio to the 'no window' ratio. Because the measurement is done *in situ* and in the location of window alignment the transmittance is known without requiring a uniformity mapping. The trap was removed for the radiometer's calibration cycles. A typical window transmittance was 0.999 921 with an uncertainty on the ratio measurements of 0.0012% at 633 nm.

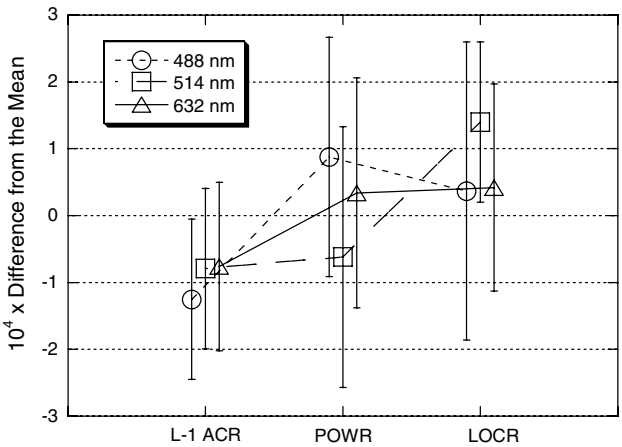

Figure 5. Results of a comparison of three cryogenic radiometers measuring a trap detector, presented in terms of the difference from the mean of the measured. The error bars show the combined standard uncertainty for the radiometers' measurements ($k = 1$).

The same traps measured by POWR were measured by other cryogenic radiometers at NIST and the calibrations agreed within 0.01% to 0.02%, which are well within the three radiometers' combined standard uncertainties (figure 5). One radiometer was the Laser Optimized Cryogenic Radiometer (LOCR) [6] located at NIST Boulder while the other radiometer is called the L-1 ACR, which is associated with the spectral irradiance and radiance responsivity calibrations with uniform sources (SIRCUS) [7] facilities at NIST Gaithersburg. A full discussion of this intercomparison will be published later.

5. Benefits and future possibilities

The evolving detector module demonstrates the benefits of the modular design. While the design, construction and wiring of each detector module required days of work, the actual exchange of detector modules in the cryostat itself took several hours. The largest time component in the exchange was the disconnection and connection of the vacuum system. A connectorized detector module was easily replaced in the cryostat.

The cost of alternative detector modules is based on the design of the receiver cavity and the procurement of the parts. The parts required to change a detector module are a heat sink, receiver cavity, electrical connectors, wiring and thermometers. This is more economical than purchasing a new radiometer for each specified power level or wavelength range.

Additional improvements are planned to the present setup of POWR. The presented uncertainties were based on measurements completed at power levels of 160 mW. To achieve these lower uncertainties at the microwatt laser intensities, POWR has been constructed with elements to address the thermal drift of the background and the noise levels of the lower signals. POWR has a temperature-controlled window section to reduce the thermal infrared drift. Also, using the phase-sensitive detection will also contribute to lowering the uncertainties of the microwatt power levels. In addition, there are plans to extend the operation of POWR in the infrared and ultraviolet. POWR is installed adjacent to the SIRCUS facilities and these have tunable lasers available

as a resource. POWR would be able to access the tunable laser resource from 200 nm to 12 µm at different intensity levels. These additional laser lines are to be brought over to POWR by fibre optic cables or light pipes. In order to measure at the various wavelengths or power levels, several receiver cavities may be required to have optimized, lower uncertainty measurements.

Plans to use POWR for irradiance measurements are being discussed. In order to change POWR to handle irradiance measurements, a detector module needs to be designed, an aperture built and measured for area, and the front optics section changed. One of the most difficult elements in that list is achieving the desired uncertainties in the aperture area measurement at cryogenic temperatures.

6. Conclusion

A new NIST reference cryogenic radiometer, POWR, has been developed. The goal in the development of POWR was to have versatility in design so that detector modules could be exchanged while providing optical power measurements at uncertainties of 0.01% or better. Final characterization measurements on Detector Module 3 are soon to be completed. In the future, POWR, using different detector modules, will be able to address special requests for measurements at different power levels or wavelengths and be able to incorporate new technologies.

Acknowledgments

We would like to thank Steven Lorentz and Joe O'Connell for their contributions in the development and construction of POWR. Responsivity measurements from the L1 ACR were provided by Steve Brown and Keith Lykke and for the LOCR by David Livigni of NIST Boulder. We would like to thank Albert C Parr, Chief of the Optical Technology Division at NIST, for his continued support of this project.

References

[1] Gentile T R, Houston J M, Hardis J E, Cromer C L and Parr A C 1996 National Institute of Standards and Technology high-accuracy cryogenic radiometer *Appl. Opt.* **35** 1056–68

[2] Gentile T R, Houston J M and Cromer C L 1996 Realization of a scale of absolute spectral response using the National Institute of Standards and Technology high-accuracy cryogenic radiometer *Appl. Opt.* **35** 4392–403

[3] Rice J P, Lorentz S R and Jung T M 1999 The next generation of active cavity radiometers for space based remote sensing *Proc. 10th Conf. on Atmospheric Radiation (28 June–2 July 1999)* preprint volume (American Meteorological Society) pp 85–8

[4] Lawrence G M, Rottman G, Harder J and Woods T 2000 Solar total irradiance monitor (TIM) *Metrologia* **37** 407–10

[5] Barnes P Y and Hsia J J 1995 45/0 reflectance factors of pressed polytetrafluoroethylene (PTFE) powder *NIST Technical Note* 1413

[6] Livigni D J, Cromer C L, Scott T R, Johnson B C and Zhang Z M 1998 Thermal characterizations of a cryogenic radiometer and comparison with a laser calorimeter *Metrologia* **35** 819–27

[7] Brown S W, Eppeldauer G P, Rice J P, Zhang J and Lykke K R 2004 Spectral irradiance and radiance responsivity calibrations using uniform sources (SIRCUS) facility at NIST *Proc. SPIE on Earth Observing Systems IX* **5542** 363–74